

Optical and morphological characterization of nanostructured AgO thin films

Adeleh Granmayeh Rad^{1*}, Hamed Abbasi²

¹Department of Basic Science, Roudehen branch, Islamic Azad University, Tehran, Iran.

²Center for Optical Diagnostics and Therapy, Department of Otorhinolaryngology, Erasmus MC Cancer Institute, Rotterdam, Netherlands.

*Corresponding author: granmayeh.r@gmail.com

Received 9 October 2022; Accepted 8 November 2022; Published online 15 November 2022

Abstract:

Silver oxide (AgO) thin films were prepared by using a cylindrical direct current reactive magnetron sputtering system at 10^{-5} torr initial pressure on BK7 glass substrate. Samples deposited for 3, 5 and 7 minutes. Surface characterization of AgO thin films in the nanometer scale can be accurately determined using the atomic force microscopy (AFM) and X-ray diffraction (XRD). The average roughness (R_{avg}), maximum peak to valley height (R_t) and root mean square (R_{rms}) roughness are used to analyze the surface morphology of AgO films. The linear optical absorption data were measured in the visible-near infrared spectral regions and the nonlinear refractive index (n_2) of thin films is evaluated by the moiré deflectometry technique. The investigation indicates that, increase in AgO thickness leads to reduction in nonlinear refractive index.

Keywords: Silver oxide thin film; Optical property; Surface morphology; Nonlinear refractive index; Moiré deflectometry

1. Introduction

In recent years the study of new metal oxide nanomaterials thin films deposited on glass substrates has drawn a lot of attentions [1, 2] because of their optical response [3], applications in biomedicine [4] and energy storage [5]. Also, accurate control of oxide thin film synthesis and processing is important in a variety of technological applications including micro sensors, microelectronics, and catalysis [6–8]. Therefore, they are made from every class of material and by different processes including sol gel processing, atomic layer deposition, physical and chemical vapor deposition techniques to meet such varied needs [9]. Different parameters of films, such as thickness, grain size, etc. play a significant role to characterize them in the length scale from nano to micro. [10]. Being able to probe dynamic process of thin film surfaces, the knowledge of the topographic surface maps at nanometric resolution is essential [11, 12]. The surface roughness of transparent conductive thin films has a substantial effect on device performance [13]. The growth of new deposited thin films compounds, such as semiconductors, allows us to get more nonlinear optical characteristics of such structures [14]. It is well known that

composited thin films due to their potential applications in optoelectronics as optical limiters and optical switches are noticed.

Various techniques have been developed to characterize the nonlinear refractive index of nano materials. In some context to show the strong nonlinearity response of materials in nano scales, various laser power density has applied [15–19]. Several studies have revealed nonlinearity of nanoparticles thin films [20], as well as nanoparticles colloids [21], and dyes doped liquid crystal [22], by Moiré deflectometry [23] technique. The basic constituents of a Moiré deflectometer are a collimated light source and a pair of linear transmission gratings, preferably of a Gaussian wave profile.

This study focuses on nanostructured silver oxide thin films. Silver is a one of the most applicable metallic materials. Every interested person can find numerous applications of these nanoparticles in different types (e.g. colloids, thin films, etc.) [24]. This nanostructured silver oxide thin film has been applied successfully as a substrate for Surface Enhanced Raman Spectroscopy (SERS) to detect of molecular level [25]. Different shapes of their oxides' crystal structures make them suitable for various optical and electrical applications [26]. Silver oxide nanomaterials have been

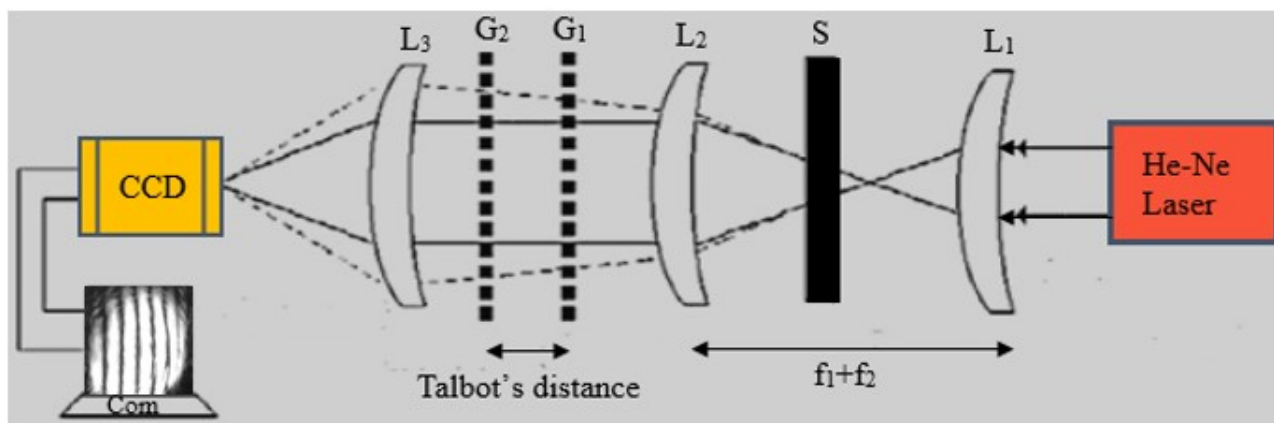


Figure 1. Schematic set-up of the Moiré deflectometry technique. L₁, focusing lens; S, sample; L₂, collimating lens; G₁, first grating; G₂, second grating; L₃, Fourier transforming lens; Com, Computer.

reviewed and found to be highly conductive, that makes them appropriate for battery cell applications [27, 28], and good thermal stability, good conductivity [28–30], making them suitable for pseudo capacitor applications [31]. The aim of the present work is to study the effect of various deposition time on surface morphology, topography and texture of AgO films by atomic force microscopy. A complete surface analysis of AgO thin films using parameters such as the average roughness, total amplitude roughness, root mean square roughness is made. These are parameters that allow insight into the surface properties and quality. The nonlinear refractive index of AgO thin films was measured by Moiré deflectometry technique and the results presented.

2. Experimental details

2.1 Preparation of samples

AgO thin films were prepared by using a cylindrical direct current reactive magnetron sputtering system at 10⁻⁵ torr initial pressure on BK7 glass substrate. Pure silver was used as the target. The working gas was 99.999 % pure argon. The distance between the target and substrate is kept at 30 mm. The difference of voltages was about 2 kV, while discharge current was 30 mA. A uniform magnetic field of 400 Gauss was generated by a solenoid which was parallel to the axis of cylindrical chamber. Before deposition, BK7 glasses which were selected as substrate were cleaned using ultrasonic waves in acetone and alcohol, and finally dried by blowing air. Deposition times are 3, 5 and 7 minutes. During deposition process, no external heat was provided. The thickness of samples was carefully determined using contact measurement technique (Dektak 3 Profilometer). The thickness of samples deposited for 3 min: S1, 5 min: S2 and 7 min: S3, were measured 71.5 nm, 75.7 nm and 98.0 nm, respectively.

2.2 XRD analysis

An X-ray diffractometer (STOE), equipped with a thin film attachment unit was used to study the crystallinity of the films. The common method of analyzing materials based on

XRD pattern is using picks of XRDs graph and calculating, to find out what materials exist in the sample. These calculations are found in [32]. A simpler and faster method of analyzing materials based on XRD pattern is using software. In present work this has been done by “X, Pert” software. The features of the diffractometer were: focusing size of 1.0 × 10.0 mm, scanning mode of 2θ, scanning interval of 100° – 800°, scanning speed (2θ) of 0.1 °/min, and scanning step (2θ) of 0.01°.

2.3 AFM analysis of the surface morphology and roughness

The tapping scans were performed with an Atomic force microscopic (AFM; Park Scientific Instruments, Auto Probe cp) on an area of 1 μm and 1 μm, with a scanning speed of 0.3 Hz and a resolution of 512 pixels.

2.4 Optical properties

The VIS-IR optical absorption spectra of AgO thin films were recorded in the region 400-800 nm by a spectrophotometer (UNICO UV-2100).

The Moiré deflectometry technique was applied to measure the nonlinear refractive index of the nanostructured AgO thin films. Figure 1 shows a schematic setup for Moiré deflectometry. A low level laser beam was focused by lens L₁ and is re-collimated by lens L₂. For construction the Moiré fringe patterns, two similar transmission gratings G₁ and G₂ with a pitch of 0.1 mm were used. The distance between gratings G₁ and G₂ is important, which it must be one of the Talbot distances of the used gratings. The Talbot's distances are given by $Z(t) = tp^2/\lambda$, where p is the periodicity of the grating; λ is the wavelength of laser beam, and t is an integer. Therefore, the Moiré fringes were observed on a screen that was attached to the second grating. The Moiré fringe patterns were projected onto a computerized CCD camera by lens L₃, placed at the back of the second grating and analyzed with a software. The CCD is equipped with a variable aperture diaphragm to avoid CCD saturation.

The refractive index, n , which depends on a nonlinear lens induced by a laser beam with a spatially nonuniform intensity distribution I , due to the nonlinear additive to the refractive index is written as:

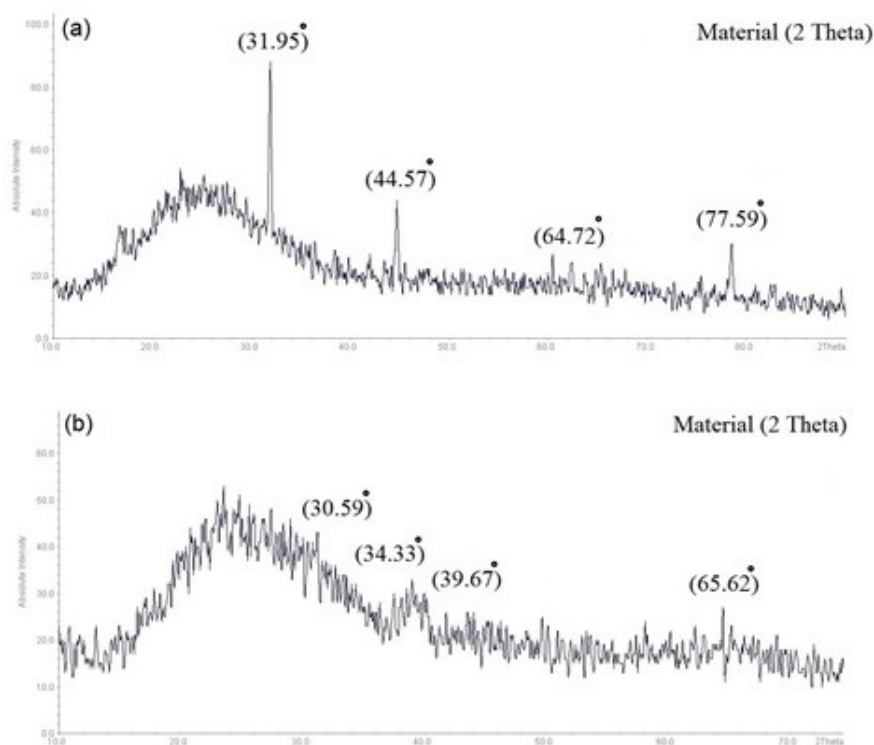


Figure 2. XRD pattern of AgO thin films. (a) is for 3-minute sample; (b) is for 5 and 7-minutes samples.

$$n(r, z) = n_0 + n_2 I(r, z) = n_0 + \Delta n(r, z) \tag{1}$$

where the linear refractive index is n_0 , the irradiance of the laser beam within the sample is $I(r, z)$, and the light-induced refractive index change is $\Delta n(r, z)$. Considering a Gaussian beam propagation through the sample in the +z direction, we will have:

$$I = I_0 \left(\frac{\omega_0^2}{\omega^2(z)} \right) e^{-\frac{2r^2}{\omega^2(z)}} \tag{2}$$

The beam waist at the focal point ($z=0$) is ω_0 , the radial

distance away from the axis is r , and $\omega(z)$ is the beam radius at a distance z from the position of the waist; $\omega(z) = \omega_0 [1 + z^2/z_0^2]^{1/2}$. Where $Z_0 = \pi \omega_0^2 / \lambda$ is an expression for the Rayleigh range of Gaussian beam, and λ is the wavelength. The irradiance of the beam at the focal point is denoted by I_0 and in terms of the input laser power, p_{in} , $I_0 = 2p_{in} / \pi \omega_0^2$. Thus, for a Gaussian laser beam propagation through the sample, the radial dependence of the irradiance, gives rise to a radially dependent parabolic refractive index change near the beam

Table 1. XRD data of Ag/Ag_xO thin films .

Sample	Phase	Peak Position (2θ)(degree)	(hkl)	Crystal System	Ref. Code
S1	AgO	31.95	(1,1,1)	Cubic	[00-043-1038]
S1	Ag	44.57	(2,0,0)	Cubic	[00-087-0718]
S1	Ag	64.72	(2,2,0)	Cubic	[00-087-0598]
S1	Ag	77.59	(3,1,1)	Cubic	[00-087-0718]
S2	AgO	30.59	(1,1,0)	Monoclinic	[01-080-1269]
S2	AgO	34.33	(0,0,2)	Monoclinic	[00-074-1750]
S2	AgO	39.67	(2,0,2)	Monoclinic	[00-074-1750]
S2	Ag ₂ O	65.62	(3,1,1)	Cubic	[00-076-1393]
S3	AgO	30.78	(1,1,0)	Monoclinic	[01-080-1269]
S3	AgO	34.16	(0,0,2)	Monoclinic	[00-074-1750]
S3	AgO	39.38	(2,0,2)	Monoclinic	[00-074-1750]
S3	Ag ₂ O	65.57	(3,1,1)	Cubic	[00-076-1393]

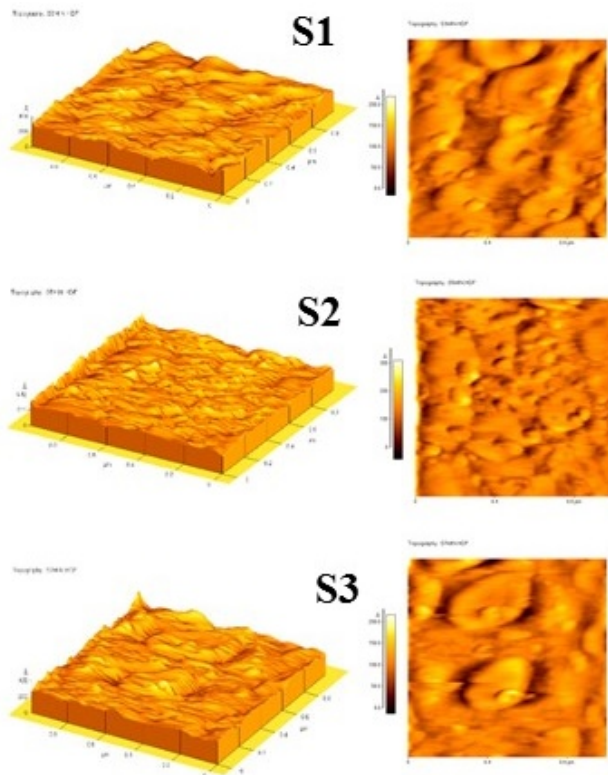


Figure 3. Surface morphology of thin films by AFM analysis.

axis. That is:

$$\Delta n = n_2 I_0 \left(\frac{\omega_0^2}{\omega^2(z)} \right) e^{-\frac{2r^2}{\omega^2(z)}} \quad (3)$$

Then, using the transmission phase function of a positive thin lens [33], as a result, the lowest nonlinear refractive index for the nonlinear medium of thickness d , can be written as:

$$n_{2,min} = \frac{\theta}{2z_t} \left(\frac{f_2^2 \pi \omega_0^4}{2d p_{in} z_0^2} \right) \alpha_{min} \quad (4)$$

where α_{min} is minimum angle of rotation and f_2 is focal length of second lens. Moving the sample along the propagation path led to variations of the effective focal length of the sample that can be measured from the amount of fringes rotation angle.

3. Results and discussion

3.1 XRD analysis of AgO thin films

Depending on the time of deposition and the amount of oxygen in the chamber, the whole or some amounts of the deposited silver may change to silver oxide. The more time is devoted to deposit, the chance of silver oxide to be deposited would be more. This fact can be observed in XRD patterns of thin films, deposited in various time durations. 3-min deposited sample contain both silver and silver oxide, while 5-min and 7- min deposited samples contain only silver oxide (Fig. 2). X-ray diffraction of the silver oxide films treated in oxygen plasma at different times showed

Table 2. The roughness of AgO thin films by AFM analysis.

Sample	Thickness (nm)	Roughness Parameters (nm)		
		R_t	R_{rms}	R_{avg}
S1	71.5	23.7	2.65	2.13
S2	75.7	35.4	3.37	2.52
S3	98.0	52.1	8.11	6.54

three major broad X-ray diffraction peaks at $2\theta = 31.95$, 44.57 and 77.59 respectively, for sample 1. The strong diffraction peaks at $2\theta = 31.95$ related to Bragg reflections of AgO according to JCPDS [00-043-1038]. For sample 2 and 3, there are four major X-ray diffraction peaks at $2\theta = 30.59$, 34.33 , 39.67 and 65.62 respectively and the strong peak at $2\theta = 39.67$ is related to monoclinic AgO according to JCPDS [00-074-1750] (Table.1).

3.2 AFM analysis of the surface morphology and roughness

An influential quantitatively measurement of the nanostructured surface roughness is Atomic Force Microscopy analysis. By AFM analysis of samples S1, S2 and S3 the roughness (Table. 2) and surface morphology (Fig. 3) were measured. The AFM operating mode was Contact mode. The main parameters of AFM analysis is the parameters which give information about many physical properties of film surface including morphology, surface texture and roughness values.

The total amplitude roughness (R_t) is the maximum peak height to valley depth of the surface profile. The mean surface roughness (R_{avg}) is the absolute arithmetic average relative to the base sampling length. It is effective parameter is applied to determine compliance of equipment with various industry standards. Root mean square (RMS) roughness (R_{rms}) is the square root of the distribution of surface height recorded within the evaluation length. It shows the standard deviation of the profile heights. It is remarkable that R_{rms} is more sensitive than average surface roughness. These numerical parameters are important to describe and classify surface of the same type.

AFM analysis of the surface morphology and roughness of AgO thin film, S1, with 3-minute deposition time, presented very low roughness of nanometer in the order $R_{avg} = 2.13$ nm, and The results obtained from the UV-VIS spectroscopy in Figure 5, show that samples have plasmonic absorption peaks at visible region. $R_{rms} = 2.65$ nm.

For samples S2 which was coated by 5-minute deposition time, AFM surface analysis showed an increase in roughness to $R_{avg} = 2.52$ nm, and $R_{rms} = 3.37$ nm. In the case of sample S3 fabricated by 7- minute deposition time, the AFM analysis revealed higher roughness of $R_{avg} = 6.54$ nm and $R_{rms} = 8.11$ nm.

Based on parameters obtained from samples, the roughness increases with the amount of AgO in the coating that AFM analysis showed this results. The overall roughness of the surface, R_t is increased by increasing the thickness of thin

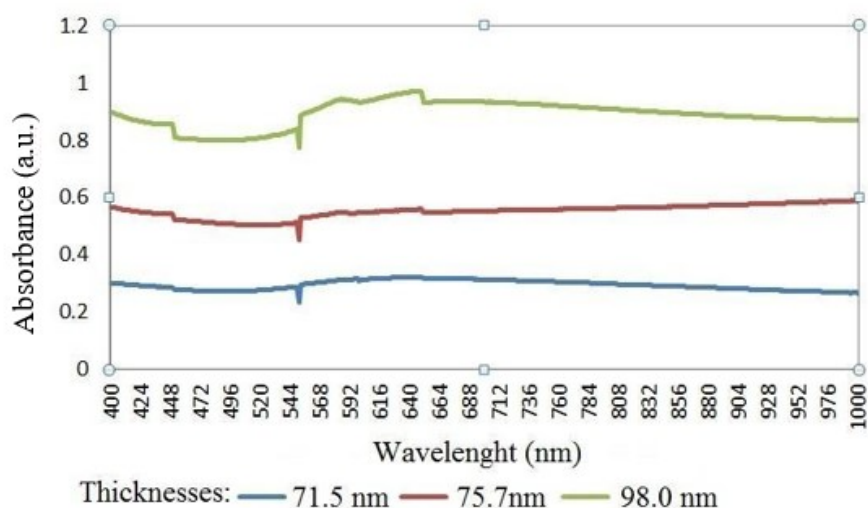


Figure 4. Absorption spectrum of AgO thin films (from VIS to NIR).

films.

3.3 Optical properties

For determination the linear characteristics of AgO thin films We used the UV-VIS spectroscopy. Fig. 4 shows the absorption spectrum of the samples with different thicknesses. The spectra were symmetrical.

One of the purpose of this study is to calculate the nonlinear refractive index of silver thin films. Figure 5 shows the experimental setup of Moiré deflectometry was applied to measure the nonlinear refractive index of AgO thin films. To avoid the thermal effect a low level He-Ne laser ($\lambda = 632.8$ nm, 15 mW) is expanded and collimated. Two Ronchi gratings, G_1 and G_2 , with the same pitch $d = 0.1$ mm are placed in the $t = 4$ th. The Talbot's distance is $Z_{(t=4)} \approx 64$ mm. After the second grating, a convex lens is placed, and it is followed by a diaphragm. The diaphragm is placed at a focal plane of the convex lens to select the first diffraction order. The fringes pattern is monitored by a CCD camera, which is transferred and analyzed in a computer.

Moiré deflectometry is a high precision technique for measuring optical nonlinear response of materials. The accuracy of this technique is determined by the minimum rotation

angle (α_{min}) that can be measured. Figure 6 shows the rotation angle of Moiré fringes along z direction for the AgO thin film with a thickness of 71.5 nm on BK7 substrate.

Rotation of moiré fringe patterns which has been recorded along Laser beam propagation (z direction), near the focus point is shown in Fig. 7.

Based on deflection mapping of Moiré fringes patterns the distribution of the nonlinear refractive index of sample was calculated. As increasing of thickness, increasing or decreasing the nonlinear refractive index of samples depends on sample properties [34]. This experiment was applied for the samples with thickness of 71.5 nm, 75.7 nm and 98.0 nm. Results are represented in Table 3. We performed as the thickness increased the nonlinear refractive index of AgO thin films decreased. The nonlinear refraction index was measured to be of the order of 10^{-5} cm^2W^{-1} and the change in refractive index was of the order of 10^{-3} . AgO thin film of 98.0 nm thickness, indicates low nonlinear refraction response, as with an increase in the deposition time, Ag nanoparticles are placed so close to each other that there is little void between them.



Figure 5. Experimental setup of Moiré deflectometry: 1, He-Ne laser; 2, mirror; 3, spatial filter; 4 and 5 lens; 6, sample; 7, lens; 8 and 9 grating; 10, lens; 11, diaphragm; 12, CCD.

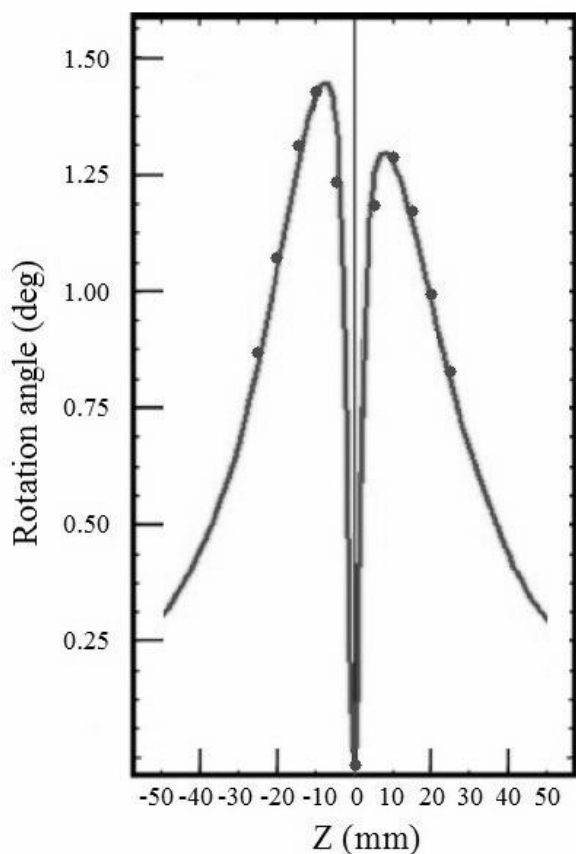


Figure 6. The moiré fringes rotation angle of silver oxide thin film at 71.5 nm thickness. The solid line is the theoretical result.

4. Conclusion

Atomic force microscopy (AFM) was applied to detect surface morphologies of AgO thin films prepared on glass substrates by DC reactive magnetron sputtering method. The thickness of samples deposited for 3 min, 5 min and 7 min, were measured 71.5 nm, 75.7 nm and 98.0 nm, Atomic force microscopy (AFM) was applied to detect surface morphologies of AgO thin films prepared on glass substrates by DC reactive magnetron sputtering method. The thickness of samples deposited for 3 min, 5 min and 7 min, were measured 71.5 nm, 75.7 nm and 98.0 nm, respectively. AFM analysis of samples showed, the roughness increases with the amount of AgO in the coating.

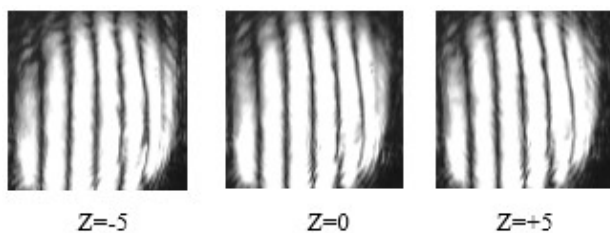


Figure 7. The Moiré fringes patterns of the silver thin film with the thickness of 71.5 nm was recorded at $z = -5$ mm, $z = 0$ and $z = +5$ mm respectively.

Table 3. Results for nonlinear refractive index of AgO thin films estimated by Moire deflectometry experiment.

Sample	Thickness (nm)	nonlinear refractive index (n_2) cm^2W^{-1}
S1	71.5	4.90×10^{-5}
S2	75.7	4.75×10^{-5}
S3	98.0	3.22×10^{-5}

The chemical composition of the deposited AgO thin films was determined by XRD analysis and the results showed that the samples were amorphous. The optical absorbance spectrum in the visible-near IR region was observed. The effect of thin film thickness on nonlinear optical properties of AgO nanostructure thin films was studied. By moiré deflectometry technique the nonlinear refractive index, n_2 , of silver oxide thin films were measured. This technique is a laser-based, high resolution technique. A low level laser to avoid thermal effects was applied. The nonlinear refractive index was measured to be of the order of $10^{-5} \text{ cm}^2 \text{ W}^{-1}$. As the thickness increased, the linear refractive index of the transparent AgO films decreased.

Conflict of interest statement

The authors declare that they have no conflict of interest.

References

- [1] S. Suren, W. Limkitnuwat, P. Benjapongvimon, and S. Kheawhom. *Thin Solid Films*, **607**:36, 2016.
- [2] M. Shahul Hameed, J. Joseph Princice, N. Ramesh Babu, and A. Arunachalam. *Journal of Materials Science: Materials in Electronics*, **28**:8675, 2017.
- [3] D. Nathiya, N. Alhaji, and A. Ayeshamariam. *Journal of Nanoscience, NanoEngineering and Applications*, **9**:46, 2019.
- [4] A. C. Burduşel, O. Gherasim, A. M. Grumezescu, L. Mogoantă, A. Ficai, and E. Andronescu. *Nanomaterials*, **8**:681, 2018.
- [5] M. Mirzaeian, A. A. Ogwu, H. F. Jirandehi, S. Aidarova, Z. Ospanova, and N. Tsendzughul. *Colloids and Surfaces A: Physicochemical and Engineering Aspects*, **519**:223, 2017.
- [6] F. Lorestani, Z. Shahnava, P. Mna, Y. Alias, and N. S. A. Manan. *Sensors and Actuators B: Chemical*, **208**:389, 2015.
- [7] M. Trivedi, G. Singh, A. Kumar, and N. P. Rath. *Inorganica Chimica Acta*, **438**:255, 2015.
- [8] F. X. Bock, T. M. Christensen, S. B. Rivers, L. D. Doucette, and R. J. Lad. *Thin Solid Films*, **468**:57, 2004.

- [9] M. Ohring. *Materials Science of Thin Films: Deposition and Structure*. Academic Press, 2th edition, 2001.
- [10] E. Acosta. *Thin Films/Properties and Applications*. London: IntechOpen, 1th edition, 2021.
- [11] K. R. Nagabhushana, B. N. Lakshminarasappa, and F. Singh. *Nuclear Instruments and Methods in Physics Research B*, **266**:1040, 2008.
- [12] M. Kwoka, L. Ottaviano, and J. Szuber. *Thin Solid Films*, **515**:8328, 2007.
- [13] G. Song, Y. Wang, and D. Q. Tan. *IET Nanodielectrics*, **5**:1, 2022.
- [14] C. N.R. Rao, G. U. Kulkarni, P. J. Thomas, and P. P. Edwards. *Chemical Society Reviews*, **29**:27, 2000.
- [15] M. Tajdidzadeh, A.B. Zakaria, A. Z. Talib, A. S. Gene, and S. Shirzadi. *Journal of Nanomaterials*, **2017**:4803843, 2017.
- [16] D. D. Smith, Y. Yoon, R. W. Boyd, J. K. Campbell, L. A. Baker, and R. M. Crooks. *Journal of Applied Physics*, **86**:6200, 1999.
- [17] R. West, Y. Wang, and T. Goodson. *The Journal of Physical Chemistry B*, **107**:3419, 2003.
- [18] A. I. Ryasnyanskiy, B. Palpant, S. Debrus, U. Pal, and A. Stepanov. *Journal of Luminescence*, **127**:181, 2007.
- [19] A. Rout, G. S. Boltaev, R. A. Ganeev, Y. Fu, S. K. Maurya, V. V. Kim, K. Srinivasa Rao, and C. Guo. *Nanomaterials*, **9**:291, 2019.
- [20] A. Granmayeh Rad, K. Madanipour, M. H. Afzali, A. Koohian, and D. Dorrnian. *Proceedings of SPIE*, **7993**:79930H, 2011.
- [21] A. Granmayeh Rad, H. Abbasi, and M. H. Afzali. *Physics Procedia*, **22**:203, 2011.
- [22] M. H. Majles Ara, S. H. Mousavi, S. Salmani, and E. Koushki. *Journal of Molecular Liquids*, **140**:21, 2008.
- [23] I. Glatt and O. Kafri. *Optics and Lasers in Engineering*, **8**:277, 1988.
- [24] A. Granmayeh Rad and H. Abbasi. *Advanced Materials Research*, **1409**:488, 2012.
- [25] D. Büchel, C. Mihalcea, and T. Fukaya. *Applied Physics Letters*, **79**:620, 2001.
- [26] A. Hammad, M. Abdel-Wahab, and A. Alshahrie. *Digest Journal of Nanomaterials and Biostructures*, **11**:1245, 2016.
- [27] S. Berchmans, A. J. Bandodkar, W. Jia, J. Ramírez, Y. S. Meng, and J. Wang. *Journal of Materials Chemistry*, **2**:15788, 2014.
- [28] X. Zhang, S. Stewart, and D. W. Shoesmith. *Journal of the Electrochemical Society*, **154**:70, 2007.
- [29] Y. Y. Evan, T. Salim, R. A. Ismail, and M. A. Fakhry. *International Journal of Nanoelectronics and Materials*, **9**:111, 2016.
- [30] A. C. Nwanya, P. E. Ugwuoke, B. A. Ezekoye, R. U. Osuji, and F. I. Ezema. *Advances in Materials Science and Engineering*, **2013**:450820, 2013.
- [31] A.I. Oje, A. A. Ogwu, M. Mirzaeian, N. Tsendzughul, and A. M. Oje. *Journal of Science: Advanced Materials and Devices*, **4**:213, 2019.
- [32] Y. Zoo, D. Adams, J. W. Mayer, and T. L. Alford. *Thin Solid Films*, **513**:170, 2006.
- [33] K. Jamshidi-Ghaleh and N. Mansour. *Optics communications*, **234**:419, 2004.
- [34] S. S Lin, Y. H. Hung, and S. C. Chen. *Thin Solid Films*, **517**:4621, 2009.